Received: 1 August 2023 | Revised: 9 November 2023 | Accepted: 4 December 2023

DOI: 10.1002/hbm.26569

RESEARCH ARTICLE

WILEY

Distinct parallel activation and interaction between dorsal and ventral pathways during phonological and semantic processing: A cTBS-fMRI study

Yudan Luo [1] | Ke Wang [1,2] | Saiyi Jiao [1] | Jiahong Zeng [1] | Zaizhu Han [1]

[1]National Key Laboratory of Cognitive Neuroscience and Learning and IDG/McGovern Institute for Brain Research, Beijing Normal University, Beijing, China

[2]School of System Science, Beijing Normal University, Beijing, China

Correspondence
Zaizhu Han, National Key Laboratory of Cognitive Neuroscience and Learning and IDG/McGovern Institute for Brain Research, Beijing Normal University, Beijing 100875, China.
Email: zzhhan@bnu.edu.cn

Funding information
National Natural Science Foundation of China, Grant/Award Numbers: 81972144, 32271091, 81870833, 82372555

Abstract

Successful visual word recognition requires the integration of phonological and semantic information, which is supported by the dorsal and ventral pathways in the brain. However, the functional specialization or interaction of these pathways during phonological and semantic processing remains unclear. Previous research has been limited by its dependence on correlational functional magnetic resonance imaging (fMRI) results or causal validation using patient populations, which are susceptible to confounds such as plasticity and lesion characteristics. To address this, the present study employed continuous theta-burst stimulation combined with fMRI in a within-subject design to assess rapid adaptation in regional activity and functional connectivity of the dorsal and ventral pathways during phonological and semantic tasks. This assessment followed the precise inhibition of the left inferior parietal lobule and anterior temporal lobe in the dorsal and ventral pathways, respectively. Our results reveal that both the dorsal and ventral pathways were activated during phonological and semantic processing, while the adaptation activation and interactive network were modulated by the task type and inhibited region. The two pathways exhibited interconnectivity in phonological processing, and disruption of either pathway led to rapid adaptation across both pathways. In contrast, only the ventral pathway exhibited connectivity in semantic processing, and disruption of this pathway alone resulted in adaptive effects primarily in the ventral pathway. These findings provide essential evidence supporting the interactive theory, phonological information processing in particular, potentially providing meaningful implications for clinical populations.

KEYWORDS
cTBS-fMRI combination, dual pathways, interactive network, phonological processing, semantic processing

Yudan Luo and Ke Wang contributed equally to this work.

Practitioner Points

- Phonological processing during word recognition involves both dorsal and ventral pathways.
- Continuous theta-burst stimulation yields diverse adaptive effects for phonological and semantic processing.
- Phonological and semantic processing exhibit distinct interactions in dual pathways.

1 | INTRODUCTION

Visual word recognition, an evolutionarily recent and influential human ability, involves the integration of phonological, semantic, and orthographic information within a neural network spanning multiple distributed brain regions (Price, 2012; Rueckl et al., 2015). The network comprises two distinctive pathways, namely the dorsal and ventral pathways (Carreiras et al., 2014; Friederici & Gierhan, 2013), which have triggered intense debates regarding their functional specialization or interaction. The *specialization theory* posits that the dorsal and ventral pathways primarily process phonological and semantic information, respectively (Coltheart et al., 2001; Rastle & Coltheart, 1999). Studies in healthy individuals have reported stronger activation of the dorsal or ventral pathways during phonological or semantic tasks, respectively (Saur et al., 2008; Yvert et al., 2012). Two crucial regions are the left inferior parietal lobule (IPL) in the dorsal pathway, which acts as a relay station for phonological conversion, and the left anterior temporal lobe (ATL) in the ventral pathway, which serves as a hub for semantic representations (Price, 2012; Taylor et al., 2013). Damage to each of these two pathways in patients caused corresponding phonology- or semantics-specific deficits (Lambon Ralph et al., 2012; Sakurai et al., 2010).

In contrast, the *interactive theory* suggests that both the dorsal and ventral pathways are involved in phonological and semantic processing during visual word recognition (Houghton & Zorzi, 2003; Plaut et al., 1996; Woollams et al., 2007). Neuroimaging studies have shown simultaneous activation of both pathways in healthy individuals (Binder et al., 2005; Levy et al., 2009; Pattamadilok et al., 2017). Patients with left IPL dysfunction develop phonological deficits and exhibit compensatory phonological encoding in the ventral and right homologous pathways (Jiao et al., 2020; Spironelli et al., 2010; Ueno & Lambon Ralph, 2013). Similarly, left ATL damage in patients leads to semantic deficits and stronger activation in dorsal regions (Wilson et al., 2009), while postoperative recovery after left ATL resection involves activity in the right inferior temporal gyrus (ITG) predicting reading ability (Noppeney et al., 2005). These findings support the simultaneous activation of the two language pathways during phonological and semantic processing in visual word recognition. However, the observed effects may be a by-product in healthy brains due to shared blood vessels and neural connections or the neuroanatomical and functional reorganization in patients due to long-term compensatory plasticity. Additionally, brain lesion studies have involved cross-sectional data, ignoring individual differences in premorbid or acute status, lesion location, or size (Benghanem et al., 2019).

Fortunately, transcranial magnetic stimulation (TMS), by mimicking lesions through temporary and precisely noninvasive stimulation, provides a valuable alternative for assessing rapid adaptation. Elucidating the potential for flexible adaptation, a widespread mechanism in brain networks, can gain crucial insights into the functional specificity and interactions between the dorsal and ventral pathways in visual word recognition (Vasileiadi et al., 2023). Inhibitory TMS over the left IPL demonstrated delayed responses in phonological tasks and reduced activation in the bilateral supramarginal gyrus (SMG) and frontal operculum (Hartwigsen et al., 2010, 2017), while the inhibitory stimulation of the left ATL led to maladaptive changes in semantic performance (Ueno et al., 2018; Woollams et al., 2017), functional activation and connectivity of the left ATL accompanied by increased right ATL activation (Jung & Lambon Ralph, 2016, 2021). However, these TMS studies may not fully resolve the theoretical dispute due to their focus on behavioral performance (Ueno et al., 2018), unclear neural alterations in both pathways (Hartwigsen et al., 2017), imprecise stimulation positions derived from other literature (Jung & Lambon Ralph, 2016), and investigation of only phonological or semantic tasks. The dynamic details of how the dorsal and ventral pathways reorganize themselves into novel functional networks for processing information across phonological and semantic domains are still unknown.

To address the aforementioned limitations, the current study employed continuous theta-burst stimulation (cTBS) to selectively inhibit the individualized left IPL and ATL regions in the dorsal and ventral pathways, respectively. Subsequently, phonological and semantic tasks were performed during functional magnetic resonance imaging (fMRI) scans. It is important to note that a sham condition without actual stimulation was included, and the precise left IPL and ATL coordinates were determined using a localizer fMRI scan. Therefore, each participant underwent three cTBS sessions and four fMRI scans (Figure 1). The comparative analysis of behavioral and neural changes was conducted between the sham and real cTBS conditions, both within and across the phonological and semantic tasks to identify the task-related and—specific activation and connectivity. The neural changes encompassed regional activity and functional connectivity (FC) of the whole brain, as well as specific regions of interest (ROIs) within the dorsal and ventral pathways in both hemispheres.

2 | MATERIALS AND METHODS

2.1 | Participants

A total of 16 healthy volunteers were recruited from Beijing, China, for this study. One of them was removed from our analyses because of incomplete data collection. All participants were native Chinese (Mandarin) speakers, with six males and an average age of 22.93

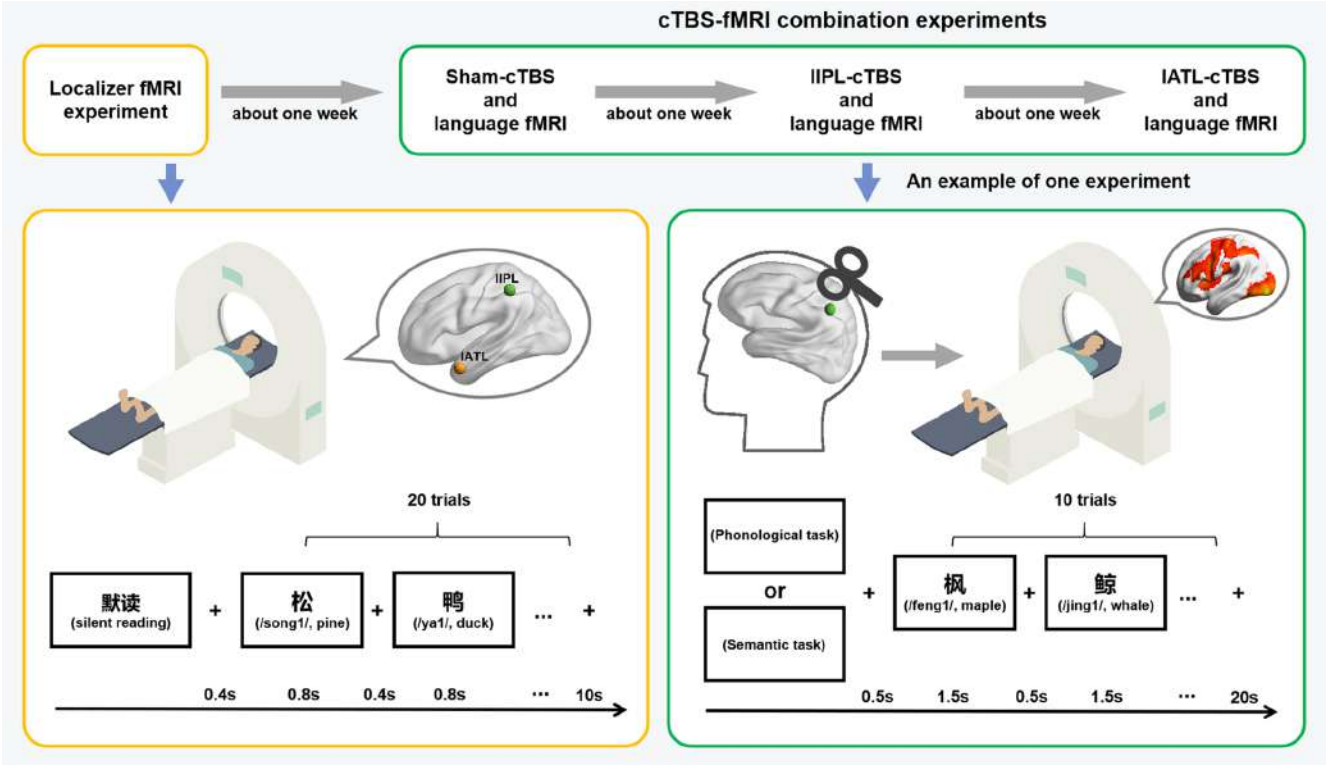

FIGURE 1 Experimental procedure and paradigm. Each participant underwent four functional magnetic resonance imaging (fMRI) scans and three continuous theta-burst stimulation (cTBS) sessions. The first fMRI scan (silent reading) precisely localized the stimulation target regions (lIPL and lATL) for each participant. Subsequently, three cTBS-fMRI experiments were conducted, with real-cTBS applied over either the lIPL or lATL, or a sham-cTBS condition without actual stimulation. This was followed by an fMRI scan during which participants performed phonological and semantic tasks. The order of the three cTBS conditions (lIPL, lATL, or sham) and the two fMRI tasks (phonological or semantic) was counterbalanced across participants in a Latin-square design. lATL: left anterior temporal lobe, lIPL: left inferior parietal lobule.

± 1.88 years. Thirteen participants were right-handed, while the remaining two were ambidextrous (Oldfield, 1971). Our localizer and main fMRI scans (see details below) showed that each subject exhibited left hemispheric dominance in language processing. All participants had normal or corrected-to-normal vision and hearing, no history of neurological or psychiatric disorders, and no contraindications for fMRI or TMS. Written informed consent was obtained from all participants, and the study was approved by the Institutional Review Board of the National Key Laboratory of Cognitive Neuroscience and Learning, Beijing Normal University.

2.2 | Stimulus and protocol

The study consisted of four experiments conducted over approximately 1 month (34.27 ± 17.32 days) (Figure 1). The first experiment involved a localizer fMRI scan to identify the target regions (left IPL and ATL) for cTBS in each participant. Subsequently, participants underwent three cTBS sessions outside the scanner, including the sham, left IPL, and left ATL stimulation conditions. Finally, participants underwent the main language experiment inside the MRI scanner. To minimize practice effects, three sets of well-matched stimuli were used for the main language task, with a minimum 1-week interval (8.97 ± 3.81 days) between experiments. All fMRI scans utilized a block design, and the order of the cTBS conditions and main-task stimulus sets were counterbalanced across participants in a Latin-square design.

2.2.1 | Localizer fMRI experiment

To accurately target the left IPL and ATL for cTBS in each participant, a localizer fMRI scan was conducted. The target regions were defined based on the contrast between regular versus scrambled (or exceptional vs. scrambled) words, as these contrasts are commonly used to define the left IPL and ATL (Hoffman et al., 2015; Wilson et al., 2009). The stimuli included 160 regular characters, 160 exceptional characters, and 80 scrambled characters. The regular and exceptional characters were well matched for frequency (202.35 ± 342.44 vs. 220.04 ± 223.47 per million occurrences), number of strokes (9.60 ± 2.58 vs. 9.74 ± 2.56), and number of logographemes (2.99 ± 0.88 vs. 2.98 ± 0.81) (*ps* >.59). Scrambled characters were created by randomly combining the cells of a character split into a 100 × 100 grid. The localizer experiment consisted of two runs, each with ten blocks. Regular, exceptional, and scrambled characters were presented in four, four, and two blocks, respectively. Each block consisted of

20 characters presented visually for 800 ms, followed by a 400 ms blank screen. Fixation blocks lasting 10 s were included between the character blocks. Participants were instructed to silently read each Chinese character in the regular and exceptional character blocks, and to silently say "/*hao3*/" (好, okay) when encountering each scrambled character in the scrambled character blocks.

2.2.2 | cTBS sessions

Neuronavigation cTBS was administered using a Magstim Rapid^2 stimulator fit with a 70-mm figure-eight coil (Magstim Company, Whitland, UK) at an intensity of 80% of the individual resting motor threshold (RMT) (Jung & Lambon Ralph, 2016; Sasaki et al., 2018). The RMT was determined as the minimum stimulation intensity at the optimal scalp position that elicited a motor-evoked potential greater than 50 μV in at least 5 of 10 consecutive trials, which were recorded using Ag/AgCl surface electrodes at the contralateral abductor pollicis brevis. Stimulation targets were determined based on the localizer fMRI scan. A continuous 600-pulse train over 40 s was administered in which three pulses at 50 Hz were repeated every 200 ms. The coil was placed tangentially on the scalp with the handle pointing posteriorly (corresponds to a posterior-to-anterior direction, Sasaki et al., 2018) for real cTBS and vertically for sham cTBS (with the pulse train emitted into the air) to control for stimulation sounds and scalp sensations. After the cTBS procedure, participants slowly moved to the fMRI scanning room and completed the fMRI scan within 1 h (51.51 ± 3.44 min). The effects of 600 pulses of cTBS were assumed to last approximately 60 min (Chung et al., 2016; Huang et al., 2005).

2.2.3 | Language fMRI experiment

The study used low-frequency inconsistent words as stimuli, similar to a previous study (Ueno et al., 2018). A total of 480 characters were selected from the UCS Chinese Character Database (Standards Press of China, 1993). To exclude the influences of sublexical regularity and transparency (Borleffs et al., 2019; Shu et al., 2003; Taylor et al., 2013), the characters were further divided into four 2-factor orthogonal conditions: two varying in regularity of phonetic radicals (low, high) and two varying in transparency of semantic radicals (low, high). The 4 conditions had the same number (each condition had 120 characters), frequency (6.44 ± 4.17 vs. 6.28 ± 4.01 vs. 6.04 ± 4.18 vs. 6.40 ± 4.51 per million of occurrences), number of strokes (10.33 ± 3.03 vs. 10.57 ± 2.79 vs. 10.68 ± 2.74 vs. 10.78 ± 3.06), and number of logographemes of characters (3.10 ± 0.92 vs. 3.22 ± 0.99 vs. 3.19 ± 0.94 vs. 3.38 ± 1.00) (*ps* > .13). The fMRI tasks included phonological and semantic decisions, with each task comprising three sets of stimuli. Each stimulus set consisted of two runs, and each run included eight blocks with 10 Chinese characters per block. Blocks were separated by a 20 s fixation period. Each character was presented visually for 1500 ms, preceded by a 500 ms fixation cross. Participants were instructed to judge whether the pronunciation of the target character (e.g., 枫, /feng1/, maple) contained a given onset (e.g., /f/) in the phonological task and whether the target character belonged to a given semantic category (e.g., plant) in the semantic task. Responses were made by pressing "YES" or "NO" buttons. Each participant completed three fMRI scans corresponding to the three cTBS conditions (sham, left IPL, and left ATL stimulation), with 32 blocks completed per scan (16 phonological and 16 semantic blocks). The order of phonological and semantic tasks was counterbalanced across participants.

2.3 | Neuroimaging data acquisition

All brain images were acquired on the same 3 T Siemens Prisma scanner (Siemens, Erlangen, Germany) at Beijing Normal University. At each time of scanning, the abovementioned task-state and resting-state fMRI data were collected from each participant. The resting-state data were not analyzed in the present study. We also collected a magnetization-prepared rapid gradient echo (MPRAGE) T1-weighted 3D structural image in the first fMRI scan. *The 3D T1-weighted images* utilized the following scanning parameters: 208 sagittal slices, slice thickness = 1 mm, repetition time (TR) = 2530 ms, echo time (TE) = 2.27 ms, flip angle = 7°, field of view (FOV) = 256 × 256 mm^2, and voxel size = 1 × 1 × 1 mm^3. *The task-related fMRI data* were obtained with an echo-planar imaging (EPI) sequence with multiband acceleration, which is a widely used technique in fMRI data collection that can dramatically reduce the acquisition time by simultaneously obtaining multiple slices (Cahart et al., 2023; Demetriou et al., 2018): 72 transverse slices, multiband factor = 3, slice thickness = 2 mm, TR = 2000 ms, TE = 34 ms, flip angle = 90°, FOV = 200 × 200 mm^2, and voxel size = 2 × 2 × 2 mm^3. Along with the EPI sequence, the following settings were used to collect *the resting-state fMRI data*: 45 transverse slices, slice thickness = 3 mm, TR = 1000 ms, TE = 30 ms, flip angle = 70°, FOV = 192 × 192 mm^2, and voxel size = 3 × 3 × 3 mm^3.

2.4 | Neuroimaging data preprocessing

The preprocessing and statistical analyses of fMRI data were carried out using standard methods with SPM12 (Wellcome Centre for Human Neuroimaging, http://www.fil.ion.ucl.ac.uk/spm). The first five images of each run were removed to ensure the initial stabilization of the fMRI signal. Slice-timing correction with the middle slice as a reference was performed to adjust for the difference in the acquisition time of the slices. Head movement was realigned with a 6-parameter rigid-body transformation. The T1-weighted image resulting after the segment was coregistered with the mean functional image was normalized to the Montreal Neurological Institute (MNI) space with a resampled voxel size of 3 × 3 × 3 mm^3. Finally, a 6 mm full-width half-maximum Gaussian kernel was used to smooth the normalized functional images, improving the signal-to-noise ratio. In the first level of analysis (the level of individuals), the functional images of two runs

were high-pass filtered with a cut-off of 128 s, and then a general linear model (GLM) was implemented with a boxcar function convolved with the canonical hemodynamic response function (HRF) to estimate the condition effect. Because of excessive head movement (translation >2 mm or rotation >2°), two runs in the phonological task from different subjects were excluded.

2.5 | Statistical analysis of localizer fMRI data

We precisely identified the two cTBS stimulation sites (left IPL and ATL) for each subject. Initially, we used the automated anatomical labeling atlas-90 (AAL-90) (Tzourio-Mazoyer et al., 2002) to create anatomical masks for the two sites. According to the AAL-90, the IPL mask consists of the left IPL, SMG, and angular gyrus (AG), while the ATL mask includes the left temporal pole and the first third of superior, middle, and inferior temporal gyri. Subsequently, the left IPL stimulation site for a subject was determined as the area exhibiting peak blood oxygenation level-dependent (BOLD) signals in the first-level contrast map between regular and scrambled characters within the IPL mask ($p < .005$, cluster size >5 voxels). The mean peak MNI coordinates across all individuals were as follows: *X*, *Y*, $Z = -52.3 \pm 11.01$, -37.2 ± 12.02, 37.2 ± 8.54 (Table 1). Similarly, the left ATL stimulation site was defined as the area with peak BOLD signals in the first-level contrast map between exceptional and scrambled characters within the ATL mask ($p < .005$, cluster size >5 voxels), with the mean peak MNI coordinates across all individuals being *X*, *Y*, $Z = -50.2 \pm 8.31$, 2.6 ± 12.66, -25.33 ± 7.83. To account for individual differences, we transformed the sites into each subject's native space using an inverse transformation from T1-weighted images normalized to the MNI template. The resulting converted sites were used as the targets for cTBS.

TABLE 1 Individualized MNI coordinates of the stimulated regions in the left IPL and ATL derived from localization fMRI experiments.

	Individual left IPL			Individual left ATL		
Subject	*X*	*Y*	*Z*	*X*	*Y*	*Z*
Sub01	−36	−39	48	−39	15	−33
Sub02	−33	−45	48	−48	5	−36
Sub03	−30	−49	45	−42	6	−33
Sub04	−63	−27	42	−42	21	−21
Sub06	−54	−21	39	−45	−18	−33
Sub07	−66	−27	27	−48	−18	−21
Sub08	−57	−24	27	−42	18	−33
Sub09	−64	−33	24	−51	6	−27
Sub10	−45	−69	27	−54	12	−18
Sub11	−51	−37	33	−64	−12	−12
Sub12	−54	−42	48	−57	−12	−15
Sub13	−63	−42	33	−53	13	−32
Sub14	−57	−24	48	−60	3	−21
Sub15	−54	−34	33	−66	−9	−15
Sub16	−57	−45	36	−42	9	−30

Abbreviations: ATL, anterior temporal lobe; IPL, inferior parietal lobule.

2.6 | Statistical analysis of language fMRI data

We investigated the rapid dynamic changes during phonological and semantic tasks under both sham and real cTBS conditions. To accomplish this, we analyzed the changes in neural activation intensity or FC across the whole brain and within language-related ROIs, providing complementary insights (Szycik et al., 2009). Each analysis was divided into two subanalyses: (1) analysis of activation intensity (or FC) in the sham condition to reveal the neural patterns of the dorsal and ventral pathways, and (2) analysis of changes in activation intensity (or FC) following real cTBS to uncover the rapid modulation in the dorsal and ventral pathways due to dysfunction in the target region. Each subanalysis involved examining the activation (or FC) of task-related and task-specific regions by comparing the values of the phonological and semantic tasks with those of the fixation (baseline) condition, as well as comparing the signals between the two tasks.

2.6.1 | Whole-brain activation intensity

Activation intensity in the sham condition

This analysis aimed to identify activation in task-related and task-specific regions during the sham condition. Task-related regions exhibited higher activation intensity values in the phonological or semantic task compared to the fixation condition, while task-specific regions showed activation intensity values that differed between the two tasks. To achieve this, we extracted the BOLD activation values of the contrast (character vs. fixation) for each voxel in each task and subject. Task-related regions were identified by comparing the intensity values in each task with zero across subjects using a *one-sample t test*. We corrected for multiple comparisons using the false discovery rate (*FDR*) (voxel-level $p_{FDR} < .05$, cluster size >50 voxels). Task-specific regions were identified by comparing the activation intensity between the two tasks using a *paired-sample t test* (voxel-level $p_{FDR} < .05$ and cluster size >50 voxels).

Change in activation intensity after real cTBS

This analysis aimed to identify changes in the activation of task-related and task-specific regions following real cTBS compared to sham cTBS. For each real cTBS condition, we extracted the activation intensity values of the contrast (real vs. sham cTBS) for each voxel in each task and subject. Task-related regions were identified by comparing the intensity values in each task with zero across subjects (voxel-level $p_{FDR} < .05$ and cluster size >50 voxels). Task-specific regions were identified by comparing the intensity values between the two tasks across subjects (voxel-level $p_{FDR} < .05$ and cluster size >50 voxels).

2.6.2 | Activation intensity in the language-relevant ROIs

For each subject, we determined the two left ROIs (left IPL, left ATL) that received real cTBS, as well as their corresponding right homologous ROIs (right IPL, right ATL). The other language-related ROIs were derived from the activation intensity map of the whole brain in the sham condition. The procedure involved extracting the peak activation in each cluster for the task-related and task-specific regions that reached significance (voxel-level p_{FDR} <.0005 and cluster size >50 voxels). If multiple peaks appeared in the same AAL region, the average coordinates of the peaks were recorded as the peak AAL region. Consequently, each AAL region had at most one language ROI. Each ROI was created as a sphere with a radius of 9 mm centered on the stimulated site or the peak coordinates.

Activation intensity in the sham condition

First, for each task, we extracted the mean BOLD activation value of the contrast (character vs. fixation) across voxels in each ROI for each subject. Then, we compared the mean activation values of each ROI in each task with zero across subjects to identify the task-related ROIs. Finally, we compared the mean activation values of each ROI between the two tasks across subjects to identify the task-specific ROIs.

Change in activation intensity after real cTBS

The task-related and task-specific regions were identified using the same procedure as above, replacing the mean BOLD activation values of the contrast between the character and fixation condition with those of the contrast between real and sham cTBS.

2.6.3 | Functional Connectivity between stimulation ROIs and other language-relevant ROIs

All the ROIs mentioned above were included in the FC analysis. We applied data-driven psychophysiological interaction (PPI) analysis (Friston et al., 1997) to identify task-related or task-specific FC between each real cTBS target and the other language-relevant ROIs.

FC in the sham condition

We extracted the BOLD time series value of sham conditions in each target ROI for each subject in each task using the SPM12 PPI Toolbox. This value was deconvolved into an estimate of the physiological variable. A psychological variable was created by convolving the conditions of interest (character = 1, fixation = −1) at each time point with a canonical HRF. The PPI was defined as the product of the mean-centered estimate of the physiological and psychological variables. The interaction value was estimated using a GLM based on the three PPI variables mentioned above, with head motion considered as a covariate. The resulting value represented the FC strength between the target ROI and the other ROI in each task. To determine whether the FC was task-related or task-specific, we compared the FC strength values of each task with zero across subjects or compared the FC strength values of one task with those of the other task across subjects.

Change in FC after real cTBS

We extracted the FC strength values of each pair (i.e., FC between the real cTBS target and other language-related ROIs) for each subject and task in the sham condition. Following the same procedure, we obtained the FC strength values of each pair in the real cTBS condition. The change in FC for each pair was calculated as the difference in FC strength between the real cTBS and sham conditions. Finally, we identified task-related and task-specific FC by comparing the difference scores of each task with zero across subjects and between the two tasks, respectively.

3 | RESULTS

3.1 | Behavioral performance

3.1.1 | Behavioral performance in the sham condition

In the sham condition, the mean accuracies of subjects ($N = 15$) in the phonological (84% ± 5%) and semantic (87% ± 6%) tasks were comparable ($t_{(14)} = -1.74$, $p > .10$). However, the mean reaction times in the phonological task (851.46 ± 121.51 ms) were significantly longer ($t_{(14)} = 9.75$, $p < .001$) than those in the semantic task (726.16 ± 119.17 ms). Participants responded slower in the phonological task compared to the semantic task under normal conditions, consistent with previous literature (Gold & Buckner, 2002).

3.1.2 | Change in behavioral performance after left IPL stimulation

Compared to the sham condition, left IPL stimulation did not lead to significant changes in the mean accuracies of the phonological task ($t_{(14)} = 0.15$, $p > .88$) or the semantic task ($t_{(14)} < 0.001$, $p > .99$), nor significant differences in accuracy between the two tasks ($t_{(14)} = 0.15$, $p > .88$). Regarding mean reaction times, there were no significant changes observed in the phonological task ($t_{(14)} = -0.15$, $p > .88$) or semantic task ($t_{(14)} = -1.05$, $p > .31$), and no significant differences in reaction times between the two tasks ($t_{(14)} = 0.88$, $p > .39$).

3.1.3 | Change in behavioral performance after left ATL stimulation

Compared to the sham condition, left ATL stimulation did not result in significant changes in the mean accuracies of the phonological ($t_{(14)} = 1.35$, $p > .20$) or semantic ($t_{(14)} < 0.39$, $p > .70$), and the difference between the two tasks ($t_{(14)} = 1.89$, $p > .08$) was not significant

(Figure 2). Regarding mean reaction times, there were no significant changes observed in either of the two tasks (phonological: $t_{(14)} = -0.78$, $p > .45$; semantic: $t_{(14)} = -0.21$, $p > .83$), and no significant differences in reaction times between the two tasks ($t_{(14)} = -0.90$, $p > .38$).

In brief, our findings indicate that transient dysfunction of the left IPL and ATL did not lead to significant behavioral changes in either the phonological or semantic task.

3.2 | Activation intensity in the whole brain

3.2.1 | Activation intensity in the sham condition

We identified five phonological-related regions with significantly higher activation intensities in the character condition compared to the fixation condition of the phonological task ($p_{FDR} < .05$, cluster size >50 voxels) (Figure 3a). These regions were distributed in both the dorsal and ventral pathways. Three regions were identified in the dorsal pathway: the right inferior frontal gyrus (IFG: *X Y Z* = 42 6 27, $t = 6.43$, 69 voxels); the right middle frontal gyrus (*X Y Z* = 39 33 24, $t = 4.76$, 77 voxels); and a region (*X Y Z* = −3 6 57, $t = 9.92$, 3744 voxels) encompassing the left supplementary motor area (SMA), precentral gyrus (PrCG), and IPL. Two regions were identified in the ventral pathway: the left lingual gyrus (LG)/fusiform gyrus (FuG)/ITG (*X Y Z* = −36 −87 −12, $t = 13.25$, 1165 voxels) and the right middle occipital gyrus/FuG/ITG (*X Y Z* = 30 −90 3, $t = 13.23$, 938 voxels). Eight semantic-related regions were activated, showing significantly higher activation intensities in the character condition compared to the fixation condition of the semantic task ($p_{FDR} < 0.05$, cluster size >50 voxels) (Figure 3b). These regions were distributed in both the dorsal and ventral pathways. Five regions were part of the dorsal pathway: the left postcentral gyrus (PoCG: *X Y Z* = −57 −18 24, $t = 4.85$, 57 voxels), the right AG (*X Y Z* = 30 −57 45, $t = 4.28$, 73 voxels), the right IFG (*X Y Z* = 39 6 27, $t = 5.78$, 119 voxels), the right insula (INS)/putamen (*X Y Z* = 33 21 6, $t = 7.70$, 607 voxels), and the right SMA/middle cingulate gyrus (*X Y Z* = 9 15 45, $t = 14.84$, 759 voxels). Two regions were in the ventral pathway: the right hippocampus (*X Y Z* = 30 −33 3, $t = 5.34$, 62 voxels) and the right inferior occipital gyrus (IOG)/FuG/ITG (*X Y Z* = 36 −84 −6, $t = 11.03$, 1078 voxels). One region (*X Y Z* = −36 −87 −12, $t = 11.60$, 4287 voxels), including the left LG, PrCG, and IFG, participated in both the left dorsal and ventral pathways. Three phonological-specific regions were identified, showing significantly higher activation intensities in the phonological task compared to the semantic task ($p < .005$, cluster size >30 voxels) (Figure 3c). These regions were the left IFG (*X Y Z* = −51 9 12, $t = 5.46$, 45 voxels), IPL (*X Y Z* = −39 −42 42, $t = 4.83$, 32 voxels), and SMA (*X Y Z* = −9 3 60, $t = 6.17$, 45 voxels), all located in the left dorsal pathway. Two semantic-specific regions were identified, showing significantly higher activation intensities in the semantic task compared to the phonological task ($p_{FDR} < .05$, cluster size >50 voxels). These regions were the left middle temporal gyrus (MTG: *X Y Z* = −54 −42 −3, $t = -8.44$, 105 voxels) and orbital gyrus (OrG: *X Y Z* = −45 48–15, $t = -8.29$, 212 voxels), both located in the left ventral pathway.

3.2.2 | Change in activation intensity after left IPL stimulation

Eight phonological-related regions were identified, exhibiting significantly different activation intensities in the left IPL stimulation condition compared to the sham condition ($p < .005$, cluster size >30 voxels) (Figure 4a). Four regions (left AG: *X Y Z* = −54 −57 30, $t = 6.42$, 134 voxels; left superior frontal gyrus: *X Y Z* = −12 63 24, $t = 5.40$, 70 voxels; left SMG: *X Y Z* = −54 −27 33, $t = 6.70$, 142 voxels; right SMA: *X Y Z* = 12 −21 48, $t = 6.07$, 35 voxels) belonged to the bilateral dorsal pathway, while three regions (Heschl's gyrus: *X Y Z* = −48 −15 9, $t = 4.52$, 32 voxels; MTG: *X Y Z* = −57 −27 −6, $t = 6.82$, 115 voxels; OrG: *X Y Z* = −36 27 −6, $t = 5.27$, 30 voxels) were part of the left ventral pathway. The remaining region (right superior temporal gyrus [STG]/PoCG: *X Y Z* = 69 −15 15, $t = 5.53$, 321 voxels) was involved in both the right dorsal and ventral pathways. No semantic-related regions were identified. Three

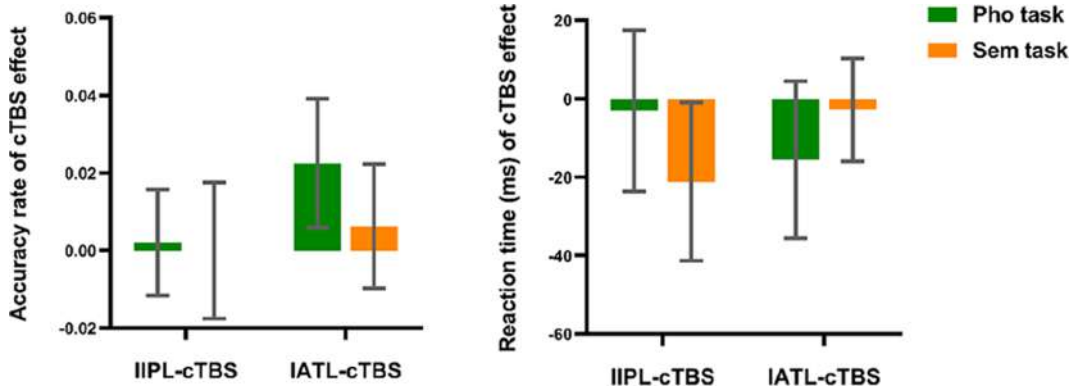

FIGURE 2 Change in task performance after real cTBS. The error bars represent standard errors. lATL, left anterior temporal lobe; lIPL, left inferior parietal lobule; pho, phonological; sem, semantic.

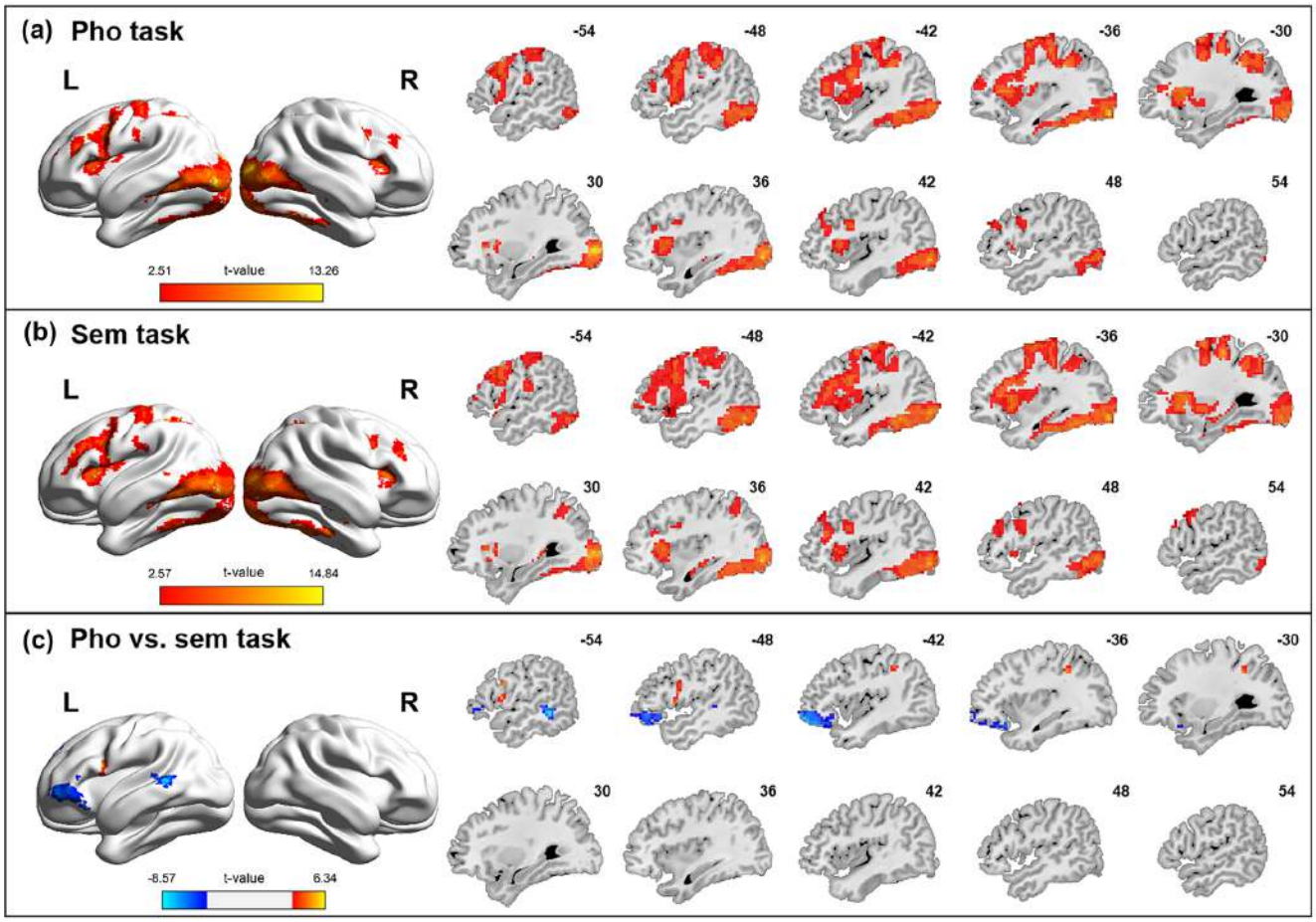

FIGURE 3 Whole-brain activation intensity maps across tasks in the sham condition. Activation intensity in the sham condition for the contrast of all words over fixation in (a) phonological task and (b) semantic task, and (c) the comparison between two tasks. L, left; pho, phonological; R, right; sem, semantic.

phonological-specific regions showed significantly greater differences in activation intensities between the sham and left IPL stimulation conditions in the phonological task compared to the semantic task ($p < .005$, cluster size >30 voxels). These regions were the left dorsal PrCG (*X Y Z* = −42 −12 51, $t = 4.69$, 34 voxels), left ventral rolandic operculum (ROL: *X Y Z* = −51 −12 15, $t = 6.26$, 96 voxels), and right STG (*X Y Z* = 66 6 −3, $t = 5.77$, 85 voxels). No semantic-specific regions were identified. Disruption of the left IPL led to adaptive activation in the bilateral dorsal and ventral pathways during the phonological task but not during the semantic task. Additionally, the left dorsal and bilateral ventral pathways exhibited greater adaptive activation in the phonological task compared to the semantic task.

3.2.3 | Change in activation intensity after left ATL stimulation

Eleven phonological-related regions were identified, exhibiting significant differences in activation intensities between the left ATL stimulation condition and the sham condition ($p < .005$, cluster size >30 voxels) (Figure 4b). These regions were distributed in both the bilateral dorsal (left INS/SMG: *X Y Z* = −39 3 −6, $t = 6.48$, 377 voxels; left PoCG: *X Y Z* = −30 −36 51, $t = 5.41$, 113 voxels; right cuneus: *X Y Z* = 12 −69 33, $t = 6.91$, 247 voxels; right PoCG/PrCG/SMG: *X Y Z* = 51 −15 42, $t = 6.80$, 985 voxels; right SMA: *X Y Z* = 9 −3 45, $t = 5.23$, 136 voxels) and ventral (left ITG: *X Y Z* = −45 −63 −6, $t = 8.20$, 46 voxels; left LG: *X Y Z* = −21 −48 −9, $t = 7.06$, 190 voxels; left MOG: *X Y Z* = −27 −84 39, $t = 5.15$, 95 voxels; left MTG: *X Y Z* = −48 −21 −12, $t = 4.37$, 37 voxels; left STG: *X Y Z* = −60 −48 15, $t = 5.82$, 78 voxels; right FuG: *X Y Z* = 33 −45 −12, $t = 6.65$, 215 voxels) pathways. Only one semantic-related region (ventral right ROL: *X Y Z* = 45 3 9, $t = 4.57$, 47 voxels) showed significant differences in activation intensities between the left ATL stimulation condition and the sham condition ($p < .005$, cluster size >30 voxels). A phonological-specific region was also identified, with significantly greater differences in activation intensities between the sham and left ATL stimulation conditions during the phonological task compared to the semantic task ($p < .005$, cluster size >30 voxels). This region (*X Y Z* = −30 −84 42, $t = 5.45$, 46 voxels) was the IPL in the left dorsal pathway. No semantic-specific region was observed. Dysfunction of the left ATL primarily affected the bilateral dorsal and ventral pathways in the phonological task, while only the right ventral pathway

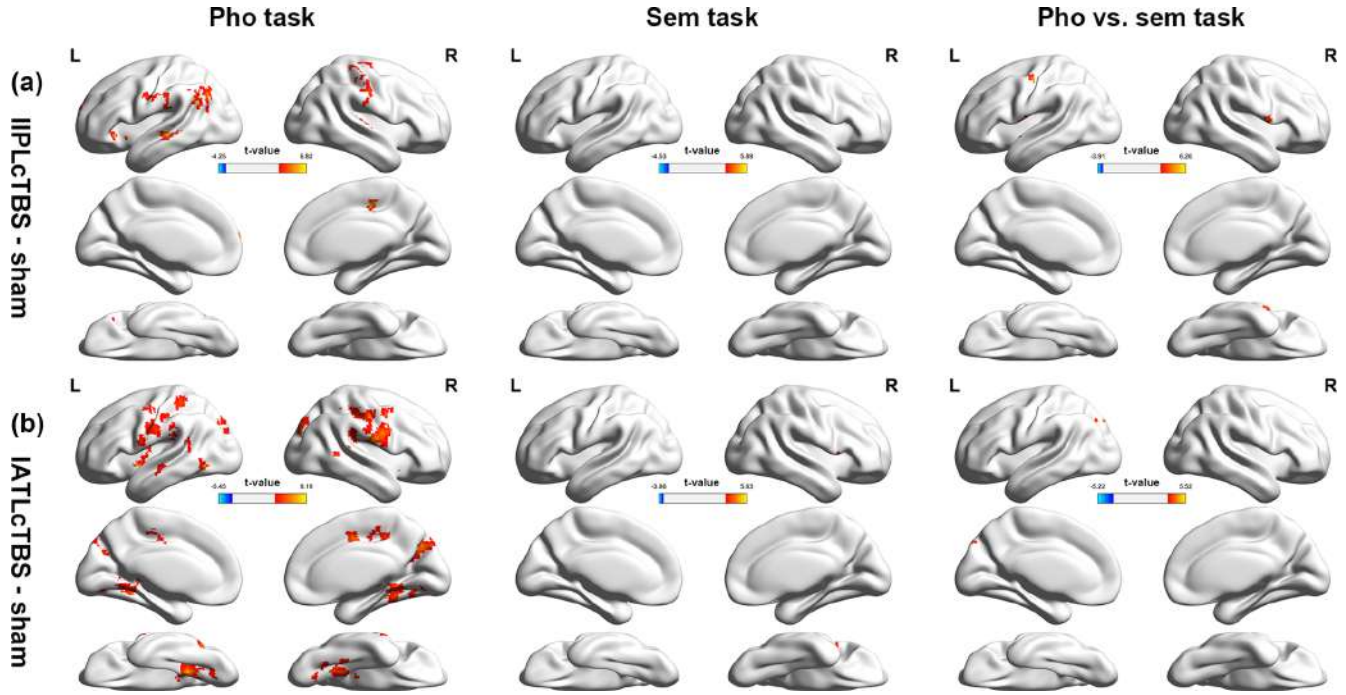

FIGURE 4 Regions displaying changes in activation intensity across tasks following real cTBS. L, left; R, right; lATL, left anterior temporal lobe; lIPL, left inferior parietal lobule; pho, phonological; sem, semantic.

was affected in the semantic task. Particularly, the IPL in the left dorsal pathway exhibited more robust adaptive activation in the phonological task compared to the semantic task.

The above results indicate that bilateral ventral and dorsal pathways involved in visual word recognition were simultaneously activated regardless of the task. The activation strength of the two pathways was modulated by the task: the phonological task preferentially activated the left dorsal pathway, while the semantic task preferentially activated the left ventral pathway. These findings align with previous research (Carreiras et al., 2014; Gold et al., 2005; Rueckl et al., 2015). Furthermore, disruption of the left IPL and ATL had a greater impact on phonological performance than semantic performance. They induced adaptive changes in the activation of the bilateral ventral and dorsal pathways, particularly the left dorsal pathway, during the phonological task. However, the influence of left ATL dysfunction on semantic performance was observed only in the right ventral pathway.

3.3 | Activation intensity in the language-relevant ROIs

In addition to the four ROIs associated with real cTBS (the bilateral IPL and ATL), nine ROIs associated with language processing were identified based on fMRI data in the sham condition (Figure 5a, Table 2). These 13 ROIs were distributed in the bilateral dorsal (6 ROIs: left INS, IFG, SMA, and IPL; right SMA, and IPL) and ventral pathways (7 ROIs: left OrG, ATL, MTG, FuG, and LG; right ATL, and IOG).

3.3.1 | Activation intensity in the sham condition

Thirteen phonological-related regions and ten semantic-related regions were identified (Figure 5b). These regions were located in the bilateral dorsal ($ts_{(14)} > 2.08$, $ps < .06$) and ventral ($ts_{(14)} > 4$, $ps < .002$) pathways. Four phonological-specific regions were observed. These regions (INS, IFG, SMA, and IPL; $ts_{(14)} > 2.20$, $ps < .05$) were in the left dorsal pathway. Four semantic-specific regions were also identified (OrG, ATL, MTG, and FuG; $ts_{(14)} > 1.89$, $ps < .08$), located in the left ventral pathway. Both phonological and semantic tasks engage the dorsal and ventral pathways, with the phonological task preferentially activating the left dorsal pathway and the semantic task preferentially activating the left ventral pathway, confirmed by earlier whole-brain analysis.

3.3.2 | Change in activation intensity after left IPL stimulation

Four phonological-related regions (left OrG, left ATL, left MTG, and right ATL; $ts_{(14)} > 2.11$, $ps < .05$) were distributed in the bilateral ventral pathways (Figure 5c). However, no semantic-related regions were identified. Three phonological-specific regions (left OrG, left ATL, and right ATL; $ts_{(14)} > 1.90$, $ps < .08$) were located in the bilateral ventral pathways. No semantic-specific regions were observed. These results indicate that dysfunction of the dorsal left IPL led to increased adaptive activity in the bilateral ventral pathways during the phonological task, while it did not cause changes in regional activation during the semantic task.

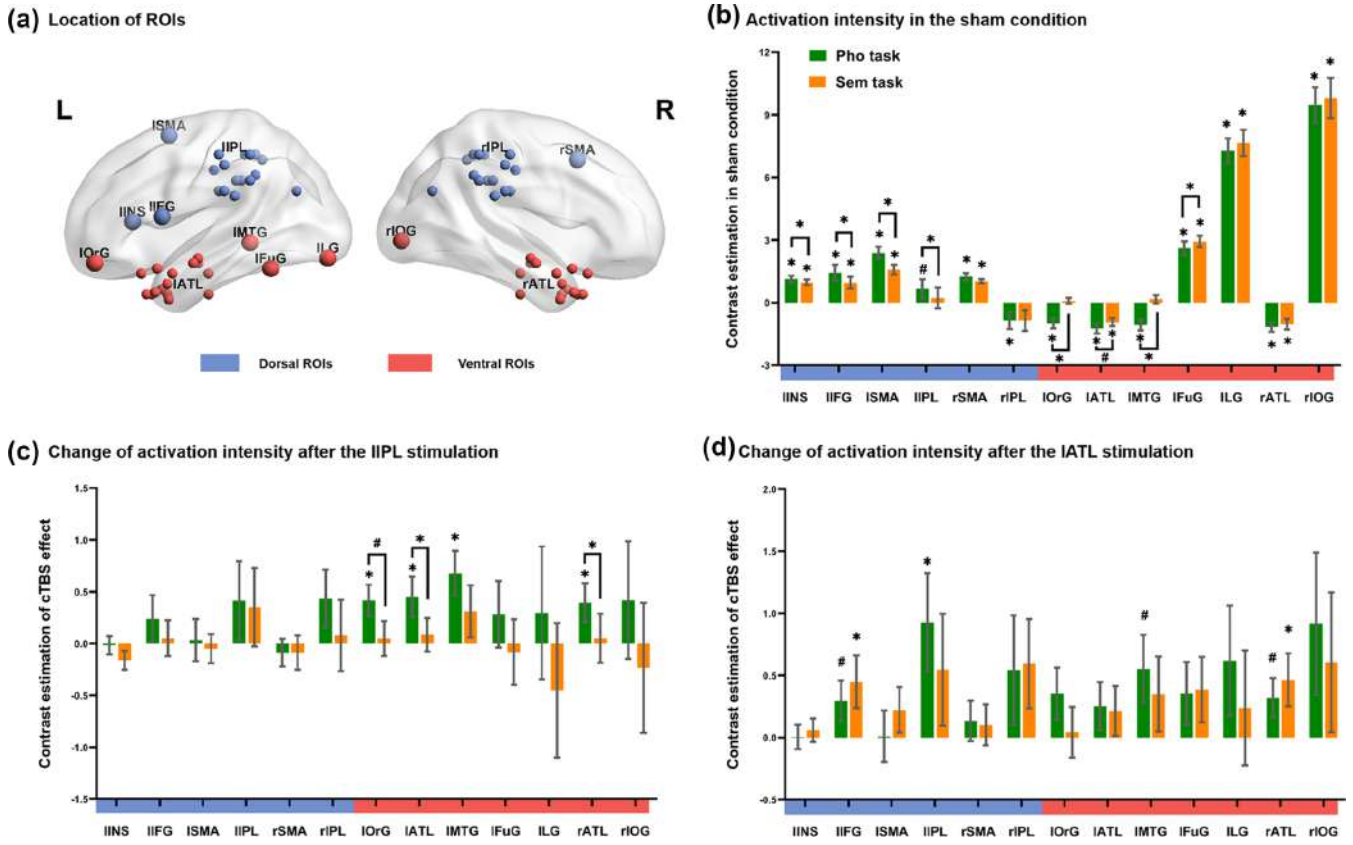

FIGURE 5 Defined regions of interest (ROIs) and their activation intensity values across tasks in different continuous theta-burst stimulation (cTBS) conditions. The error bars represent standard errors ($^{*}p < .05$, $^{\#}p < .10$). The ROIs of the dorsal or ventral pathways in each hemisphere are ordered according to their y-axis coordinate values. The full names of the ROIs are given in Table 2. Pho, phonological; sem, semantic.

TABLE 2 Defined ROIs and the MNI coordinates of their peaks.

	Pho task[a]			Sem task[a]			Pho vs. sem task[bc]			Mean value		
ROI	***X***	***Y***	***Z***	***X***	***Y***	***Z***	***X***	***Y***	***Z***	***X***	***Y***	***Z***
Dorsal pathway												
Left inferior frontal gyrus (lIFG)	–			–			−51	9	12	−51	9	12
Left insula (lINS)	−33	27	12	−27	24	6	–			−30	26	9
Left supplementary motor area (lSMA)	−3	6	57	–			−9	3	60	−6	5	59
Right supplementary motor area (rSMA)	–			9	15	45	–			9	15	45
Ventral pathway												
Left fusiform gyrus (lFuG)	−39	−54	−18	–			–			−39	−54	−18
Left lingual gyrus (lLG)	−36	−87	−12	−36	−87	−12	–			−36	−87	−12
Left middle temporal gyrus (lMTG)	–			–			−54	−42	−3	−54	−42	−3
Left orbital gyrus (lOrG)	–			–			−45	48	−15	−45	48	−15
Right inferior occipital gyrus (rIOG)	30	−90	3	36	−84	−6	–			33	−87	−2

Note: The threshold value was set to [a] $p_{FDR} < .0005$, cluster size >50 voxels, [b] Pho < Sem $p_{FDR} < .05$, cluster size >50 voxels or [c] Pho > Sem $p < .005$, cluster size >30 voxels.
Abbreviations: Pho, phonological; ROI, region of interest; sem, semantic.

3.3.3 | Change in activation intensity after left ATL stimulation

Four phonological-related regions were located in the left dorsal (IPL and IFG; $ts_{(14)} > 1.80$, $ps < .09$) and bilateral ventral (left MTG and right ATL; $ts_{(14)} > 2.02$, $ps < .06$) pathways (Figure 5d). Two semantic-related regions were the left IFG ($t_{(14)} = 2.14$, $p = .05$) in the left dorsal pathway and the right homologous region (rATL, $t_{(14)} = 2.17$, $p = .05$) in the ventral pathway. No phonological- or semantic-specific regions were identified. These results indicate that ventral left ATL

disruption caused compensatory activity in the left dorsal regions (e.g., left IFG) and the right homologous regions (e.g., right ATL), regardless of the task.

In essence, the ROI analysis replicated the findings from the whole-brain analysis, with a novel result being that disruption of the left ATL led to semantic adaptive activation in the left dorsal pathway.

3.4 | FC between stimulation ROIs and other language-relevant ROIs

Thirteen ROIs were examined, including the two stimulation ROIs (left IPL or ATL). Thus, we investigated 12 FCs from each stimulation ROI to the other 12 ROIs and 24 FCs from the two stimulation ROIs. The task-relatedness and specificity of these 24 FCs in the sham and real cTBS conditions were examined.

3.4.1 | FC in the sham condition

Seven out of twenty-four connections were phonological-related, showing FC values in the character condition that were significantly or marginally different from those in the fixation condition (Figure 6a). These connectivity pairs included two pairs of regions within the dorsal pathway (hereafter, intra-FC), one pair of regions within the ventral pathway (intra-FC), and four pairs of regions where one region was located in the dorsal pathway and the other in the ventral pathway (hereafter, inter-FC). The two dorsal intra-FCs were the left IPL-right IPL ($t_{(14)} = 2.36$, $p = .03$) and left IPL-SMA ($t_{(14)} = 2.40$, $p = .03$). The ventral intra-FC was the left ATL-right ATL ($t_{(14)} = 2.59$, $p = .02$). The four inter-FCs were the left IPL–ATL ($t_{(14)} = 2.58$, $p = .02$); left IPL-MTG ($t_{(14)} = 1.93$, $p = .07$); left IPL-FuG ($t_{(14)} = 2.40$, $p = .03$); and left IPL-right ATL ($t_{(14)} = 2.29$, $p = .04$). Two semantic-related FCs were identified, both ventral intra-FCs: the left ATL-MTG ($t_{(14)} = 2.80$, $p = .01$) and left ATL-right ATL ($t_{(14)} = 3.27$, $p = .01$).

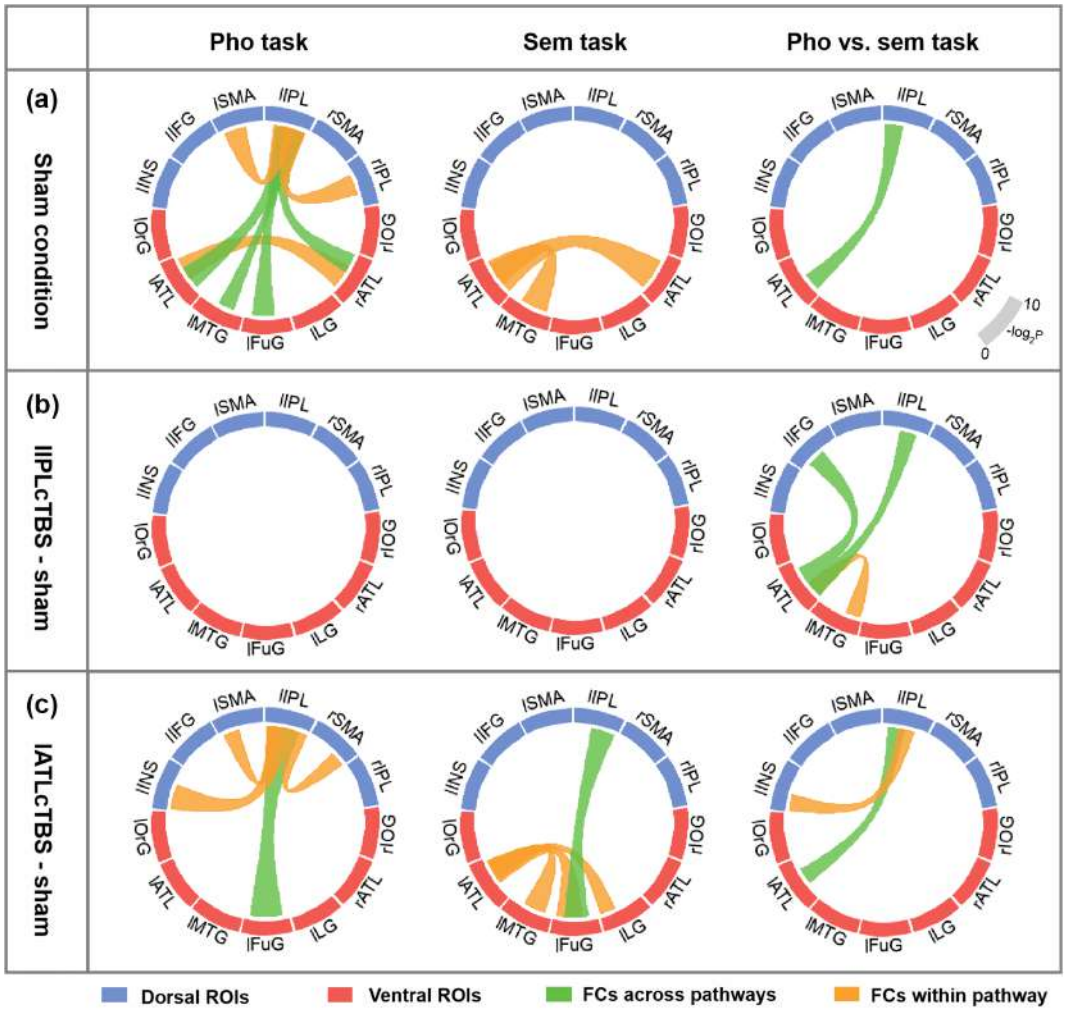

FIGURE 6 Functional connectivity between the stimulated regions of interest (ROIs) and other language-relevant ROIs across tasks in different continuous theta-burst stimulation (cTBS) conditions. The thickness of the chords represents the significance ($p < .10$) of the connectivity between the two brain areas. The thicker the chord, the lower the p value of the connectivity. The ROIs of the dorsal or ventral pathways in each hemisphere are ordered based on their y-axis coordinate values. The full names of the ROIs are provided in Table 2. FC, functional connectivity; pho, phonological; ROI, region of interest; sem, semantic.

One phonological-specific FC exhibited marginally higher differences in FC between the character and fixation condition of the phonological task compared to the semantic task. This was the left IPL–ATL ($t_{(14)} = 2.06$, $p = .06$). No semantic-specific FCs were observed. Semantic processing seems to primarily involve ventral intra-FCs, while phonological processing additionally involves dorsal intra-FCs and inter-FCs. Moreover, phonological processing induces stronger inter-FCs between the two cTBS sites.

3.4.2 | Change in FC after left IPL stimulation

We did not observe any phonological- or semantic-related FCs. Similarly, we did not find any semantic-specific FCs. However, we did find three phonological-specific FCs that showed significantly or marginally higher FC differences between the sham condition and the left-IPL-cTBS condition of the phonological task compared to the semantic task (Figure 6b). Two of these FCs were inter-FCs: the left ATL-IPL ($t_{(14)} = 2.01$, $p = .06$) and left ATL-IFG ($t_{(14)} = 2.20$, $p = .04$). The remaining ventral intra-FC was the left ATL-MTG ($t_{(14)} = 1.84$, $p = .09$). Dysfunction in the left IPL region increased the strength of ventral intra- and inter-FCs in the phonological task to a greater extent than in the semantic task.

3.4.3 | Change in FC after left ATL stimulation

We observed four phonological-related FCs that showed significantly or marginally higher FC values in the left ATL stimulation condition compared to the sham condition (Figure 6c). Three of these FCs were dorsal intra-FCs (left IPL-INS: $t_{(14)} = 2.67$, $p = .02$; left IPL-SMA: $t_{(14)} = 1.91$, $p = .08$; left IPL-right SMA: $t_{(14)} = 1.86$, $p = .08$). The remaining one was an inter-FC (left IPL-FuG: $t_{(14)} = 3.27$, $p = .01$). We also identified four semantic-related FCs, three of which were ventral intra-FCs (left ATL-MTG: $t_{(14)} = 2.40$, $p = .03$; left ATL-FuG: $t_{(14)} = 2.72$, $p = .02$; left ATL-LG: $t_{(14)} = 1.91$, $p = .08$). The remaining one was an inter-FC (left IPL-FuG: $t_{(14)} = 2.59$, $p = .02$). We found two phonological-specific FCs with FC differences between the sham and left ATL stimulation conditions of the phonological task that were marginally higher than those of the semantic task. One was the left dorsal intra-FC (left IPL-INS: $t_{(14)} = 1.95$, $p = .07$), and the other was an inter-FC (left IPL–ATL: $t_{(14)} = 2.02$, $p = .06$). No semantic-specific FCs were found. Dysfunction of the left ATL region increased the strength of dorsal intra- and inter-FCs in the phonological task and ventral intra- and inter-FCs in the semantic task, with the greater enhancement of dorsal intra- and inter-FCs in the phonological task compared to the semantic task.

To sum up, the FC results mentioned above suggest that the phonological task primarily relies on both dorsal and ventral pathways, while the semantic task primarily relies on the ventral pathway. The main difference between the two tasks lies in the inter-FC between the left dorsal and ventral pathways. Dysfunction in a critical region within one pathway led to a greater adaptive enhancement of FCs within the other pathway and across the two pathways in the phonological task compared to the semantic task. In other words, FC strength was modulated by the task type: the phonological task elicited stronger inter-FCs than the semantic task.

4 | DISCUSSION

To investigate the functional dissociation or interaction between the dorsal and ventral pathways during visual word recognition, we conducted four fMRI scans and three cTBS sessions in this study. The initial fMRI scan localized individualized critical regions in the dorsal and ventral pathways, which were then disrupted using cTBS. After stimulation, subjects performed phonological and semantic tasks during fMRI scans. Our findings revealed the coactivation of two pathways during both phonological and semantic tasks. Furthermore, the adaptation activation and dynamic network were influenced by the task type and inhibited region. The key brain regions of the dorsal and ventral pathways have direct connections in phonological tasks. Therefore, when one pathway was "damaged," the other pathway exhibited adaptive activation for the phonological processing. In contrast, the network for semantic information processing is mainly located in the ventral pathway, and only "damage" to the ventral pathway resulted in adaptive activation of the right ventral regions and left IFG for the semantic task. These findings provided robust evidence supporting the interactive theory of visual word recognition, especially in phonological information processing.

4.1 | Parallel activation and enhanced adaptation of the dual pathways in phonological processing

In the left hemisphere, both the dorsal and ventral pathways were activated during the phonological task, consistent with previous research (Binder et al., 2005; Levy et al., 2009). Interconnection between the two pathways supported a dual-pathway framework that accounts for the simultaneous yet distinct extraction of mappings from phonological-sound representations to semantic statistical structures (Hoffman et al., 2015; Pattamadilok et al., 2017; Ueno et al., 2011). Retrieving semantic information, especially for low-frequency words, facilitates phonological processing (Protopapas et al., 2016; Woollams et al., 2017). This provides preliminary support for the interactive theory that both the dorsal and ventral pathways are involved in phonological processing, rather than the specialization theory that phonology only engages the dorsal pathway. fMRI alone only provides correlational evidence for parallel processing. Our cTBS-fMRI experiment showed the genuine parallel occurrence of dual pathways, with left IPL and ATL stimulation increasing activation in the ventral and dorsal regions, respectively. These results indicate that the two pathways are not mutually exclusive but can reoptimize processing to facilitate spontaneous recovery (Borghesani et al., 2020; Klaus et al., 2020), providing further evidence for the interaction theory. When a language-related brain area within one pathway becomes

dysfunctional, the other pathway flexibly adapts by increasing both activation and connectivity to ensure successful information processing (Hartwigsen, 2018; Stefaniak et al., 2020). This could account for the absence of any alteration in our behavioral performance.

In the right hemisphere, the dorsal and ventral pathways also were robustly utilized during phonological task, with significant connectivity between the left and right regions. The left-lateralized dorsal pathway is commonly associated with language processing, while the right dorsal pathway may contribute to other phonological components (Liebenthal et al., 2013; Sammler et al., 2015). The ventral pathway is engaged bilaterally and serves as the lexical interface for abstract word representations (Hickok & Poeppel, 2007; Leonard & Chang, 2014). No adaptive activation in the right IPL was observed in our ROI analysis, but whole-brain analysis revealed increased activation in right dorsal areas after real cTBS sessions. This aligns with research on the compensatory role of the right homologous area following left IPL damage (Jiao et al., 2020) and TMS studies highlighting the critical role of bilateral IPL in phonological processing (Hartwigsen et al., 2010). Notably, cTBS over both left IPL and ATL increased right ATL activation. Higher right ATL activation in patients with left ATL resection correlated with better reading proficiency (Noppeney et al., 2005). Skilled readers can modulate the right ATL activation to enhance reading ability, consistent with our highly educated participants. Collectively, our findings support the essential role of bilateral dorsal and ventral pathways in phonological processing, highlighting their interactive and compensatory nature, and supporting the interactive theory.

4.2 | Parallel activation of the dual pathways and enhanced adaptation of the ventral pathways in semantic processing

Our study revealed bilateral dorsal and ventral pathways activation during the semantic task, with greater connectivity among the bilateral ventral regions. Additionally, cTBS only over the left ATL increased activation of the left IFG and right ventral regions and connectivity between the left ATL and other ventral regions. The validity of the interactive theory for semantic information processing is still doubtful, because no effect was observed after cTBS over the left IPL and only the ventral pathway showed adaptation effects after stimulating the left ATL. The dorsal pathway appeared relatively independent from semantic influences, potentially supporting other cognitive components like working memory or semantic control (Binder et al., 2009; Xu et al., 2017), given the low meaningfulness of the baseline condition. However, previous studies have widely confirmed the crucial role of bilateral ventral pathways in semantic information processing (Chang et al., 2015; Lambon Ralph et al., 2017). Although both pathways were engaged, the left hemisphere demonstrated greater involvement in semantic task, indicating a graded division of labor from left to right (Visser & Lambon Ralph, 2011). This can also be found in our results of increased left ATL connectivity after left ATL inactivation during the semantic task. The dorsal left IFG also played an integrative role in the language (Friederici, 2002; Lau et al., 2008) and exhibited heightened involvement in the semantic task during left ATL dysfunction. Hartwigsen and colleagues reported increased activation in dorsal posterior left IFG for semantic tasks following inhibiting key nodes in the semantic network (Hartwigsen et al., 2017). Dysfunction in a critical region may escalate task demands, prompting the engagement of broader control areas. Indeed, the human brain is organized into distributed neural networks, encompassing domain-specific and domain-general networks (Hartwigsen, 2018; Hodgson et al., 2021).

However, we found no effect during the semantic task when stimulating the left IPL, contrary to previous studies that reported compensatory activation of the ventral pathway in the presence of dorsal brain damage (Robson et al., 2014). The discrepancy may be due to differing locations of perturbations within the IPL, which comprises distinct subregions with diverse functions (Bzdok et al., 2016; Numssen et al., 2021). While the anterior dorsal IPL was inhibited in our study, the posterior ventral IPL (i.e., AG) continued to function normally. This subregion is crucial for semantic processing within the parietal lobule (Hartwigsen et al., 2017; Lambon Ralph et al., 2017). In our study, almost all of the targets (93.3%) except one were located within the phonology-related subregions, with only one target (6.7%, see Table 1 sub10) falling within the semantics-related region. This finding effectively explains why we did not observe any modulation effects in the semantic task after stimulating the left IPL. Further exploration is necessary to fully understand the role of the dorsal pathway in semantic processing.

4.3 | Differential parallel activations and interactions between dorsal and ventral pathways under the task guidance

Consistent with previous studies (Dickens et al., 2019; Taylor et al., 2013; Ueno et al., 2011), our findings indicate that the phonological task primarily activates the left dorsal pathway, whereas the semantic task primarily activates the left ventral pathway. cTBS stimulation of the left IPL enhanced activation of the left dorsal and bilateral ventral areas in the phonological task compared to the semantic task. The ventral pathway, although primarily involved in semantics, also contributes to phonological processing, particularly in individuals with expertise. Word-level information stored in the ventral pathway facilitates phonological processing (Hamilton et al., 2021; Leonard & Chang, 2014; Yi et al., 2019). This is exemplified by children relying more on the dorsal pathway during reading, while proficient adults rely more on the ventral pathway (Church et al., 2008; Provost et al., 2016). Regrettably, we did not find any brain regions where semantic effects were stronger than phonological, which might be due to the reason mentioned above, that most of the individual stimulation targets were located within the regions related to phonological processing rather than semantic processing.

Following cTBS over the left ATL, the left dorsal IPL exhibited greater activation during the phonological task than the semantic task.

The left dorsal IPL is generally considered more crucial for phonological processing, specifically in grapheme-phoneme conversion (Dickens et al., 2019; Taylor et al., 2013). Further connectivity analysis revealed the main distinction between phonological and semantic tasks: the interactive connections between the dorsal and ventral pathways. Consistent with previous findings (Battistella et al., 2019; Zheng et al., 2021), we also observed a left IPL–ATL connection during the phonological task but not the semantic task. This might also explain why stronger TMS effects were found in the dorsal pathway in the phonological task after left ATL stimulation. Because of the direct connection between the left IPL and ATL, the dorsal and ventral pathways could adapt to each other in the phonological task. Additionally, the arcuate and superior longitudinal fascicles provide the anatomical basis for the phonological information exchange between the dorsal and ventral pathways, whereas only the ventral middle and inferior longitudinal fascicles are involved in the semantic task (Saur et al., 2008, 2010). Essentially, the dorsal and ventral pathways contribute to phonological and semantic tasks. However, their functional and anatomical dissociation suggests distinct networks and diverse adaptive or compensatory effects when a critical region is inhibited.

4.4 | Limitations

The present study has several limitations. First, some weakly significant results did not survive multiple comparison corrections, likely due to the small sample size of 15 subjects. Second, the activation intensity of the simulated region did not decrease in subsequent fMRI scans, possibly attributed to the network connections facilitating information transmission and recovery of activation intensity over time (Castrillon et al., 2020). Third, focusing on phonological processing in silent reading localization tasks might have overlooked some semantic areas in ROI selection. Fourth, both phonological and semantic tasks may activate two types of information processing simultaneously, and it is difficult to get a clear-cut task response for phonological or semantic processing. Finally, the limited duration of the cTBS effect constrained the investigation to phonological and semantic information processing, neglecting other mechanisms such as orthographic and syntactic processing.

5 | CONCLUSION

Overall, by combining cTBS with fMRI scans, our study revealed the coactivation of the dorsal and ventral pathways during phonological and semantic processing in visual word recognition. Moreover, the adaptation activation and interactive network were modulated by the task type and inhibited region. These findings contribute to a better understanding of the neural mechanisms underlying visual word recognition and provide valuable evidence in support of the interactive theory especially during phonological processing, with potentially meaningful implications for clinical populations.

ACKNOWLEDGMENTS

The authors sincerely thank Dr. You Duan for his invaluable assistance with data visualization, the BNU-CN Lab members for their contributions to data collection, and all research participants for their time and cooperation. This work was supported by the National Natural Science Foundation of China (32271091, 81972144, 81870833, and 82372555).

DATA AVAILABILITY STATEMENT

The data supporting the findings of this study are available from the corresponding author (zzhhan@bnu.edu.cn) upon reasonable request.

ORCID

Zaizhu Han https://orcid.org/0000-0003-1751-6452

REFERENCES

Battistella, G., Henry, M., Gesierich, B., Wilson, S. M., Borghesani, V., Shwe, W., Miller, Z., Deleon, J., Miller, B. L., Jovicich, J., Papinutto, N., Dronkers, N. F., Seeley, W. W., Mandelli, M. L., & Gorno-Tempini, M. L. (2019). Differential intrinsic functional connectivity changes in semantic variant primary progressive aphasia. *NeuroImage: Clinical*, *22*, 101797. https://doi.org/10.1016/j.nicl.2019.101797

Benghanem, S., Rosso, C., Arbizu, C., Moulton, E., Dormont, D., Leger, A., Pires, C., & Samson, Y. (2019). Aphasia outcome: The interactions between initial severity, lesion size and location. *Journal of Neurology*, *266*(6), 1303–1309. https://doi.org/10.1007/s00415-019-09259-3

Binder, J. R., Desai, R. H., Graves, W. W., & Conant, L. L. (2009). Where is the semantic system? A critical review and meta-analysis of 120 functional neuroimaging studies. *Cerebral Cortex*, *19*(12), 2767–2796. https://doi.org/10.1093/cercor/bhp055

Binder, J. R., Medler, D. A., Desai, R., Conant, L. L., & Liebenthal, E. (2005). Some neurophysiological constraints on models of word naming. *NeuroImage*, *27*(3), 677–693. https://doi.org/10.1016/j.neuroimage.2005.04.029

Borghesani, V., Hinkley, L. B. N., Ranasinghe, K. G., Thompson, M. M. C., Shwe, W., Mizuiri, D., Lauricella, M., Europa, E., Honma, S., Miller, Z., Miller, B., Vossel, K., Henry, M. M. L., Houde, J. F., Gorno-Tempini, M. L., & Nagarajan, S. S. (2020). Taking the sublexical route: Brain dynamics of reading in the semantic variant of primary progressive aphasia. *Brain*, *143*(8), 2545–2560. https://doi.org/10.1093/brain/awaa212

Borleffs, E., Maassen, B. A. M., Lyytinen, H., & Zwarts, F. (2019). Cracking the code: The impact of orthographic transparency and morphological-syllabic complexity on reading and developmental dyslexia. *Frontiers in Psychology*, *9*, 2534.

Bzdok, D., Hartwigsen, G., Reid, A., Laird, A. R., Fox, P. T., & Eickhoff, S. B. (2016). Left inferior parietal lobe engagement in social cognition and language. *Neuroscience & Biobehavioral Reviews*, *68*, 319–334. https://doi.org/10.1016/j.neubiorev.2016.02.024

Cahart, M.-S., O'Daly, O., Giampietro, V., Timmers, M., Streffer, J., Einstein, S., Zelaya, F., Dell'Acqua, F., & Williams, S. C. R. (2023). Comparing the test–retest reliability of resting-state functional magnetic resonance imaging metrics across single band and multiband acquisitions in the context of healthy aging. *Human Brain Mapping*, *44*(5), 1901–1912. https://doi.org/10.1002/hbm.26180

Carreiras, M., Armstrong, B. C., Perea, M., & Frost, R. (2014). The what, when, where, and how of visual word recognition. *Trends in Cognitive Sciences*, *18*(2), 90–98. https://doi.org/10.1016/j.tics.2013.11.005

Castrillon, G., Sollmann, N., Kurcyus, K., Razi, A., Krieg, S. M., & Riedl, V. (2020). The physiological effects of noninvasive brain stimulation fundamentally differ across the human cortex. *Science Advances*, *6*(5), eaay2739. https://doi.org/10.1126/sciadv.aay2739

Chang, E. F., Raygor, K. P., & Berger, M. S. (2015). Contemporary model of language organization: An overview for neurosurgeons. *Journal of Neurosurgery*, *122*(2), 250–261. https://doi.org/10.3171/2014.10.JNS132647

Chung, S. W., Hill, A. T., Rogasch, N. C., Hoy, K. E., & Fitzgerald, P. B. (2016). Use of theta-burst stimulation in changing excitability of motor cortex: A systematic review and meta-analysis. *Neuroscience and Biobehavioral Reviews*, *63*, 43–64. https://doi.org/10.1016/j.neubiorev.2016.01.008

Church, J. A., Coalson, R. S., Lugar, H. M., Petersen, S. E., & Schlaggar, B. L. (2008). A developmental fMRI study of reading and repetition reveals changes in phonological and visual mechanisms over age. *Cerebral Cortex*, *18*(9), 2054–2065. https://doi.org/10.1093/cercor/bhm228

Coltheart, M., Rastle, K., Perry, C., Langdon, R., & Ziegler, J. (2001). DRC: A dual route cascaded model of visual word recognition and reading aloud. *Psychological Review*, *108*(1), 204–256. https://doi.org/10.1037/0033-295x.108.1.204

Demetriou, L., Kowalczyk, O. S., Tyson, G., Bello, T., Newbould, R. D., & Wall, M. B. (2018). A comprehensive evaluation of increasing temporal resolution with multiband-accelerated protocols and effects on statistical outcome measures in fMRI. *NeuroImage*, *176*, 404–416. https://doi.org/10.1016/j.neuroimage.2018.05.011

Dickens, J. V., Fama, M. E., DeMarco, A. T., Lacey, E. H., Friedman, R. B., & Turkeltaub, P. E. (2019). Localization of phonological and semantic contributions to reading. *The Journal of Neuroscience*, *39*(27), 5361–5368. https://doi.org/10.1523/JNEUROSCI.2707-18.2019

Friederici, A. D. (2002). Towards a neural basis of auditory sentence processing. *Trends in Cognitive Sciences*, *6*(2), 78–84. https://doi.org/10.1016/S1364-6613(00)01839-8

Friederici, A. D., & Gierhan, S. M. (2013). The language network. *Current Opinion in Neurobiology*, *23*(2), 250–254. https://doi.org/10.1016/j.conb.2012.10.002

Friston, K. J., Buechel, C., Fink, G. R., Morris, J., Rolls, E., & Dolan, R. J. (1997). Psychophysiological and modulatory interactions in neuroimaging. *NeuroImage*, *6*(3), 218–229. https://doi.org/10.1006/nimg.1997.0291

Gold, B. T., Balota, D. A., Kirchhoff, B. A., & Buckner, R. L. (2005). Common and dissociable activation patterns associated with controlled semantic and phonological processing: Evidence from FMRI adaptation. *Cerebral Cortex*, *15*(9), 1438–1450. https://doi.org/10.1093/cercor/bhi024

Gold, B. T., & Buckner, R. L. (2002). Common prefrontal regions coactivate with dissociable posterior regions during controlled semantic and phonological tasks. *Neuron*, *35*(4), 803–812. https://doi.org/10.1016/S0896-6273(02)00800-0

Hamilton, L. S., Oganian, Y., Hall, J., & Chang, E. F. (2021). Parallel and distributed encoding of speech across human auditory cortex. *Cell*, *184*(18), 4626–4639. https://doi.org/10.1016/j.cell.2021.07.019

Hartwigsen, G. (2018). Flexible redistribution in cognitive networks. *Trends in Cognitive Sciences*, *22*(8), 687–698. https://doi.org/10.1016/j.tics.2018.05.008

Hartwigsen, G., Baumgaertner, A., Price, C. J., Koehnke, M., Ulmer, S., & Siebner, H. R. (2010). Phonological decisions require both the left and right supramarginal gyri. *Proceedings of the National Academy of Sciences of the United States of America*, *107*(38), 16494–16499. https://doi.org/10.1073/pnas.1008121107

Hartwigsen, G., Bzdok, D., Klein, M., Wawrzyniak, M., Stockert, A., Wrede, K., Classen, J., & Saur, D. (2017). Rapid short-term reorganization in the language network. *eLife*, *6*, e25964. https://doi.org/10.7554/eLife.25964

Hickok, G., & Poeppel, D. (2007). The cortical organization of speech processing. *Nature Reviews. Neuroscience*, *8*(5), 393–402. https://doi.org/10.1038/nrn2113

Hodgson, V. J., Lambon Ralph, M. A., & Jackson, R. L. (2021). Multiple dimensions underlying the functional organization of the language network. *NeuroImage*, *241*, 118444. https://doi.org/10.1016/j.neuroimage.2021.118444

Hoffman, P., Lambon Ralph, M. A., & Woollams, A. M. (2015). Triangulation of the neurocomputational architecture underpinning reading aloud. *Proceedings of the National Academy of Sciences of the United States of America*, *112*(28), E3719–E3728. https://doi.org/10.1073/pnas.1502032112

Houghton, G., & Zorzi, M. (2003). Normal and impaired spelling in a connectionist dual-route architecture. *Cognitive Neuropsychology*, *20*(2), 115–162. https://doi.org/10.1080/02643290242000871

Huang, Y. Z., Edwards, M. J., Rounis, E., Bhatia, K. P., & Rothwell, J. C. (2005). Theta burst stimulation of the human motor cortex. *Neuron*, *45*(2), 201–206. https://doi.org/10.1016/j.neuron.2004.12.033

Jiao, Y., Lin, F., Wu, J., Li, H., Fu, W., Huo, R., Cao, Y., Wang, S., & Zhao, J. (2020). Plasticity in language cortex and white matter tracts after resection of dominant inferior parietal lobule arteriovenous malformations: A combined fMRI and DTI study. *Journal of Neurosurgery*, *134*(3), 953–960. https://doi.org/10.3171/2019.12.JNS191987

Jung, J., & Lambon Ralph, M. A. (2016). Mapping the dynamic network interactions underpinning cognition: A cTBS-fMRI study of the flexible adaptive neural system for semantics. *Cerebral Cortex*, *26*(8), 3580–3590. https://doi.org/10.1093/cercor/bhw149

Jung, J., & Lambon Ralph, M. A. (2021). The immediate impact of transcranial magnetic stimulation on brain structure: Short-term neuroplasticity following one session of cTBS. *NeuroImage*, *240*, 118375. https://doi.org/10.1016/j.neuroimage.2021.118375

Klaus, J., Schutter, D. J. L. G., & Piai, V. (2020). Transient perturbation of the left temporal cortex evokes plasticity-related reconfiguration of the lexical network. *Human Brain Mapping*, *41*(4), 1061–1071. https://doi.org/10.1002/hbm.24860

Lambon Ralph, M. A., Ehsan, S., Baker, G. A., & Rogers, T. T. (2012). Semantic memory is impaired in patients with unilateral anterior temporal lobe resection for temporal lobe epilepsy. *Brain*, *135*(Pt 1), 242–258. https://doi.org/10.1093/brain/awr325

Lambon Ralph, M. A., Jefferies, E., Patterson, K., & Rogers, T. T. (2017). The neural and computational bases of semantic cognition. *Nature Reviews Neuroscience*, *18*(1), 42–55. https://doi.org/10.1038/nrn.2016.150

Lau, E. F., Phillips, C., & Poeppel, D. (2008). A cortical network for semantics: (De)constructing the N400. *Nature Reviews Neuroscience*, *9*(12), 920–933. https://doi.org/10.1038/nrn2532

Leonard, M. K., & Chang, E. F. (2014). Dynamic speech representations in the human temporal lobe. *Trends in Cognitive Sciences*, *18*(9), 472–479. https://doi.org/10.1016/j.tics.2014.05.001

Levy, J., Pernet, C., Treserras, S., Boulanouar, K., Aubry, F., Démonet, J. F., & Celsis, P. (2009). Testing for the dual-route cascade reading model in the brain: An fMRI effective connectivity account of an efficient reading style. *PLoS One*, *4*(8), e6675. https://doi.org/10.1371/journal.pone.0006675

Liebenthal, E., Sabri, M., Beardsley, S. A., Mangalathu-Arumana, J., & Desai, A. (2013). Neural dynamics of phonological processing in the dorsal auditory stream. *The Journal of Neuroscience*, *33*(39), 15414–15424. https://doi.org/10.1523/JNEUROSCI.1511-13.2013

Noppeney, U., Price, C. J., Duncan, J. S., & Koepp, M. J. (2005). Reading skills after left anterior temporal lobe resection: An fMRI study. *Brain*, *128*(Pt 6), 1377–1385. https://doi.org/10.1093/brain/awh414

Numssen, O., Bzdok, D., & Hartwigsen, G. (2021). Functional specialization within the inferior parietal lobes across cognitive domains. *eLife*, *10*, e63591. https://doi.org/10.7554/eLife.63591

Oldfield, R. C. (1971). The assessment and analysis of handedness: The Edinburgh inventory. *Neuropsychologia*, *9*(1), 97–113.

Pattamadilok, C., Chanoine, V., Pallier, C., Anton, J. L., Nazarian, B., Belin, P., & Ziegler, J. C. (2017). Automaticity of phonological and semantic processing during visual word recognition. *NeuroImage*, *149*, 244–255. https://doi.org/10.1016/j.neuroimage.2017.02.003

Plaut, D. C., McClelland, J. L., Seidenberg, M. S., & Patterson, K. (1996). Understanding normal and impaired word reading: Computational principles in quasi-regular domains. *Psychological Review*, *103*(1), 56–115. https://doi.org/10.1037/0033-295X.103.1.56

Price, C. J. (2012). A review and synthesis of the first 20 years of PET and fMRI studies of heard speech, spoken language and reading. *NeuroImage*, *62*(2), 816–847. https://doi.org/10.1016/j.neuroimage.2012.04.062

Protopapas, A., Orfanidou, E., Taylor, J. S. H., Karavasilis, E., Kapnoula, E. C., Panagiotaropoulou, G., Velonakis, G., Poulou, L. S., Smyrnis, N., & Kelekis, D. (2016). Evaluating cognitive models of visual word recognition using fMRI: Effects of lexical and sublexical variables. *NeuroImage*, *128*, 328–341. https://doi.org/10.1016/j.neuroimage.2016.01.013

Provost, J. S., Brambati, S. M., Chapleau, M., & Wilson, M. A. (2016). The effect of aging on the brain network for exception word reading. *Cortex*, *84*, 90–100. https://doi.org/10.1016/j.cortex.2016.09.005

Rastle, K., & Coltheart, M. (1999). Serial and strategic effects in reading aloud. *Journal of Experimental Psychology: Human Perception and Performance*, *25*(2), 482–503. https://doi.org/10.1037/0096-1523.25.2.482

Robson, H., Zahn, R., Keidel, J. L., Binney, R. J., Sage, K., & Lambon Ralph, M. A. (2014). The anterior temporal lobes support residual comprehension in Wernicke's aphasia. *Brain*, *137*(Pt 3), 931–943. https://doi.org/10.1093/brain/awt373

Rueckl, J. G., Paz-Alonso, P. M., Molfese, P. J., Kuo, W. J., Bick, A., Frost, S. J., Hancock, R., Wu, D. H., Mencl, W. E., Duñabeitia, J. A., Lee, J. R., Oliver, M., Zevin, J. D., Hoeft, F., Carreiras, M., Tzeng, O. J. L., Pugh, K. R., & Frost, R. (2015). Universal brain signature of proficient reading: Evidence from four contrasting languages. *Proceedings of the National Academy of Sciences of the United States of America*, *112*(50), 15510–15515. https://doi.org/10.1073/pnas.1509321112

Sakurai, Y., Asami, M., & Mannen, T. (2010). Alexia and agraphia with lesions of the angular and supramarginal gyri: Evidence for the disruption of sequential processing. *Journal of the Neurological Sciences*, *288*(1–2), 25–33. https://doi.org/10.1016/j.jns.2009.10.015

Sammler, D., Grosbras, M. H., Anwander, A., Bestelmeyer, P. E. G., & Belin, P. (2015). Dorsal and ventral pathways for prosody. *Current Biology*, *25*(23), 3079–3085. https://doi.org/10.1016/j.cub.2015.10.009

Sasaki, T., Kodama, S., Togashi, N., Shirota, Y., Sugiyama, Y., Tokushige, S., Inomata-Terada, S., Terao, Y., Ugawa, Y., & Hamada, M. (2018). The intensity of continuous theta burst stimulation, but not the waveform used to elicit motor evoked potentials, influences its outcome in the human motor cortex. *Brain Stimulation*, *11*(2), 400–410. https://doi.org/10.1016/j.brs.2017.12.003

Saur, D., Kreher, B. W., Schnell, S., Kümmerer, D., Kellmeyer, P., Vry, M. S., Umarova, R., Musso, M., Glauche, V., Abel, S., Huber, W., Rijntjes, M., Hennig, J., & Weiller, C. (2008). Ventral and dorsal pathways for language. *Proceedings of the National Academy of Sciences of the United States of America*, *105*(46), 18035–18040. https://doi.org/10.1073/pnas.0805234105

Saur, D., Schelter, B., Schnell, S., Kratochvil, D., Küpper, H., Kellmeyer, P., Kümmerer, D., Klöppel, S., Glauche, V., Lange, R., Mader, W., Feess, D., Timmer, J., & Weiller, C. (2010). Combining functional and anatomical connectivity reveals brain networks for auditory language comprehension. *NeuroImage*, *49*(4), 3187–3197. https://doi.org/10.1016/j.neuroimage.2009.11.009

Shu, H., Chen, X., Anderson, R. C., Wu, N., & Xuan, Y. (2003). Properties of school Chinese: Implications for learning to read. *Child Development*, *74*(1), 27–47. https://doi.org/10.1111/1467-8624.00519

Spironelli, C., Penolazzi, B., Vio, C., & Angrilli, A. (2010). Cortical reorganization in dyslexic children after phonological training: Evidence from early evoked potentials. *Brain*, *133*(11), 3385–3395. https://doi.org/10.1093/brain/awq199

Standards Press of China. (1993). Information technology—Universal multiple-octet coded character set (UCS)—Part 1: Architecture and basic multilingual plane. Retrieved from https://std.samr.gov.cn/gb/search/gbDetailed?id=71F772D7860AD3A7E05397BE0A0AB82A

Stefaniak, J. D., Halai, A. D., & Lambon Ralph, M. A. (2020). The neural and neurocomputational bases of recovery from post-stroke aphasia. *Nature Reviews. Neurology*, *16*(1), 43–55. https://doi.org/10.1038/s41582-019-0282-1

Szycik, G. R., Jansma, H., & Münte, T. F. (2009). Audiovisual integration during speech comprehension: An fMRI study comparing ROI-based and whole brain analyses. *Human Brain Mapping*, *30*(7), 1990–1999. https://doi.org/10.1002/hbm.20640

Taylor, J. S. H., Rastle, K., & Davis, M. H. (2013). Can cognitive models explain brain activation during word and pseudoword reading? A meta-analysis of 36 neuroimaging studies. *Psychological Bulletin*, *139*(4), 766–791. https://doi.org/10.1037/a0030266

Tzourio-Mazoyer, N., Landeau, B., Papathanassiou, D., Crivello, F., Etard, O., Delcroix, N., Mazoyer, B., & Joliot, M. (2002). Automated anatomical labeling of activations in SPM using a macroscopic anatomical parcellation of the MNI MRI single-subject brain. *NeuroImage*, *15*(1), 273–289. https://doi.org/10.1006/nimg.2001.0978

Ueno, T., & Lambon Ralph, M. A. (2013). The roles of the "ventral" semantic and "dorsal" pathways in conduite d'approche: A neuroanatomically-constrained computational modeling investigation. *Frontiers in Human Neuroscience*, *7*, 422. https://doi.org/10.3389/fnhum.2013.00422

Ueno, T., Meteyard, L., Hoffman, P., & Murayama, K. (2018). The ventral anterior temporal lobe has a necessary role in exception word reading. *Cerebral Cortex*, *28*(8), 3035–3045. https://doi.org/10.1093/cercor/bhy131

Ueno, T., Saito, S., Rogers, T. T., & Lambon Ralph, M. A. (2011). Lichtheim 2: Synthesizing aphasia and the neural basis of language in a neurocomputational model of the dual dorsal-ventral language pathways. *Neuron*, *72*(2), 385–396. https://doi.org/10.1016/j.neuron.2011.09.013

Vasileiadi, M., Schuler, A.-L., Woletz, M., Linhardt, D., Windischberger, C., & Tik, M. (2023). Functional connectivity explains how neuronavigated TMS of posterior temporal subregions differentially affect language processing. *Brain Stimulation*, *16*(4), 1062–1071. https://doi.org/10.1016/j.brs.2023.06.014

Visser, M., & Lambon Ralph, M. A. (2011). Differential contributions of bilateral ventral anterior temporal lobe and left anterior superior temporal gyrus to semantic processes. *Journal of Cognitive Neuroscience*, *23*(10), 3121–3131. https://doi.org/10.1162/jocn_a_00007

Wilson, S. M., Brambati, S. M., Henry, R. G., Handwerker, D. A., Agosta, F., Miller, B. L., Wilkins, D. P., Ogar, J. M., & Gorno-Tempini, M. L. (2009). The neural basis of surface dyslexia in semantic dementia. *Brain*, *132*(1), 71–86. https://doi.org/10.1093/brain/awn300

Woollams, A. M., Lambon Ralph, M. A., Plaut, D. C., & Patterson, K. (2007). SD-squared: On the association between semantic dementia and surface dyslexia. *Psychological Review*, *114*(2), 316–339. https://doi.org/10.1037/0033-295X.114.2.316

Woollams, A. M., Madrid, G., & Lambon Ralph, M. A. (2017). Using neurostimulation to understand the impact of pre-morbid individual differences on post-lesion outcomes. *Proceedings of the National Academy of Sciences of the United States of America*, *114*(46), 12279–12284. https://doi.org/10.1073/pnas.1707162114

Xu, Y., He, Y., & Bi, Y. (2017). A tri-network model of human semantic processing. *Frontiers in Psychology*, *8*, 1538. https://doi.org/10.3389/fpsyg.2017.01538

Yi, H. G., Leonard, M. K., & Chang, E. F. (2019). The encoding of speech sounds in the superior temporal gyrus. *Neuron*, *102*(6), 1096–1110. https://doi.org/10.1016/j.neuron.2019.04.023

Yvert, G., Perrone-Bertolotti, M., Baciu, M., & David, O. (2012). Dynamic causal modeling of spatiotemporal integration of phonological and

semantic processes: An electroencephalographic study. *Journal of Neuroscience*, *32*(12), 4297–4306. https://doi.org/10.1523/JNEUROSCI.6434-11.2012

Zheng, W., Minama Reddy, G. K., Dai, F., Chandramani, A., Brang, D., Hunter, S., Kohrman, M. H., Rose, S., Rossi, M., Tao, J., Wu, S., Byrne, R., Frim, D. M., Warnke, P., & Towle, V. L. (2021). Chasing language through the brain: Successive parallel networks. *Clinical Neurophysiology*, *132*(1), 80–93. https://doi.org/10.1016/j.clinph.2020.10.007

How to cite this article: Luo, Y., Wang, K., Jiao, S., Zeng, J., & Han, Z. (2024). Distinct parallel activation and interaction between dorsal and ventral pathways during phonological and semantic processing: A cTBS-fMRI study. *Human Brain Mapping*, *45*(1), e26569. https://doi.org/10.1002/hbm.26569